Cellulose (2018) 25:6055–6069
https://doi.org/10.1007/s10570-018-1958-1

ORIGINAL PAPER

Continuous roll-to-roll coating of cellulose nanocrystals onto paperboard

Rajesh Koppolu · Tiffany Abitbol · Vinay Kumar · Aayush Kumar Jaiswal · Agne Swerin · Martti Toivakka

Received: 7 June 2018 / Accepted: 19 July 2018 / Published online: 20 July 2018

Abstract There is an increased interest in the use of cellulose nanocrystal (CNC) films and coatings for a range of functional applications in the fields of material science, biomedical engineering, and pharmaceutical sciences. Most of these applications have been demonstrated on films and coatings produced using laboratory-scale batch processes, such as solvent casting, dip coating, or spin coating. For successful coating application of CNC suspensions using a high throughput process, several challenges need to be addressed: relatively high viscosity at low solids content, coating brittleness, and potentially poor adhesion to the substrate. This work aims to address these problems. The impact of plasticizer on suspension rheology, coating adhesion, and barrier properties was quantified, and the effect of different pre-coatings on the wettability and adhesion of CNC coatings to paperboard substrates was explored. CNC suspensions were coated onto pre-coated paperboard in a roll-to-roll process using a custom-built slot die. The addition of sorbitol reduced the brittleness of the CNC coatings, and a thin cationic starch pre-coating improved their adhesion to the paperboard. The final coat weight, dry coating thickness, and coating line speed were varied between 1–11 g/m^2, 900 nm–7 μm, and 2.5–10 m/min, respectively. The barrier properties, adhesive strength, coating coverage, and smoothness of the CNC coatings were characterized. SEM images show full coating coverage at coat weights as low as 1.5 g/m^2. With sorbitol as plasticizer and at coat weights above 3.5 g/m^2, heptane vapor and water vapor transmission rates were reduced by as much as 99% and 75% respectively. Compared to other film casting techniques, the process employed in this work deposits a relatively thick coating in significantly less time, and may therefore pave the way toward various functional applications based on CNCs.

Electronic supplementary material The online version of this article (https://doi.org/10.1007/s10570-018-1958-1) contains supplementary material, which is available to authorized users.

R. Koppolu (✉) · V. Kumar · A. K. Jaiswal · M. Toivakka
Laboratory of Paper Coating and Converting, Center for Functional Materials, Åbo Akademi University, 20500 Turku, Finland
e-mail: Rajesh.Koppolu@abo.fi

T. Abitbol · A. Swerin
Bioscience and Materials – Surface, Process and Formulation, RISE Research Institutes of Sweden, 114 28 Stockholm, Sweden

A. Swerin
Division of Surface and Corrosion Science, Department of Chemistry, KTH Royal Institute of Technology, 100 44 Stockholm, Sweden

V. Kumar
High Performance Fiber Products, VTT Technical Research Center of Finland Ltd., 02044 Espoo, Finland

Graphical abstract

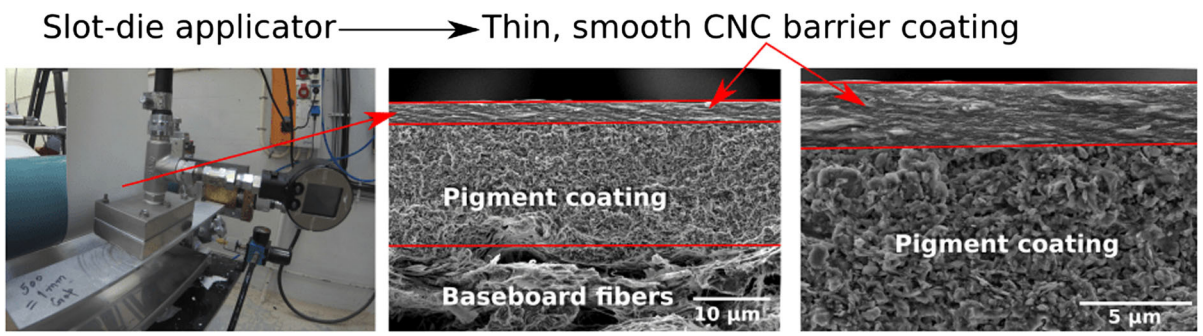

Keywords Cellulose nanocrystals (CNCs) · Slot coating · Roll-to-roll coating · Sorbitol plasticizer · Barrier properties · Barrier films

Introduction

Over the last decade, the interest in nanocellulose has increased exponentially and the list of its applications continues to grow at an accelerated pace. Nanocellulose can broadly be divided into three basic types, depending on its source, processing technique, morphology and properties: cellulose nanofibrils (CNFs), cellulose nanocrystals (CNCs), and bacterial nanocellulose (BNC) (Abitbol et al. 2016; Dufresne 2013). Many comprehensive reviews have described fundamental aspects of different types of nanocelluloses, their properties, processing methods, and applications (Abitbol et al. 2016; Brodin et al. 2014; Dufresne 2013; Eichhorn et al. 2010; Hamad 2017; Hubbe et al. 2017; Isogai 2013; Klemm et al. 2011; Lavoine et al. 2012; Lindström et al. 2015; Mariano et al. 2014; Moon et al. 2016; Osong et al. 2016; Plackett et al. 2014; Samyn et al. 2018; Habibi et al. 2010).

Generally, CNCs are produced by strong acid hydrolysis of wood cellulose pulp, with sulfuric, hydrochloric and phosphoric acids being the most commonly used acids (Nelson et al. 2016). The strong acid preferentially degrades the amorphous regions of cellulose microfibrils leaving behind crystalline cellulose nanoparticles called CNCs. The resulting CNC suspension is neutralized and any free acid molecules left in the suspension are removed by washing with water followed by successive centrifugations or by dialysis (Dufresne 2013). The morphology and crystallinity of CNC is highly influenced by the source of the raw material. Wood pulp based CNCs have widths between 5 and 20 nm, lengths between 100 and 500 nm and can reach crystallinity close to 90% (Elazzouzi-Hafraoui et al. 2007; Pan et al. 2013), while bacterial based CNCs tend to be narrower and have lengths reaching 1 µm (Feng et al. 2015).

The relatively large specific surface area together with the abundance of surface hydroxyl groups of CNCs opens up many exciting applications. CNC films and coatings provide barrier against oxygen (Feng et al. 2015; Fortunati et al. 2012; Li et al. 2013) and grease (Gicquel et al. 2017). Cellulose-based materials in general exhibit poor barrier against water vapor. Recently, Herrera et al. (2017) have shown that by adding sorbitol as a plasticizer and a citric acid cross-linker, the water vapor permeability of the resulting coatings is significantly reduced. Several research groups have also demonstrated an improvement in water vapor barrier for CNC-based composite films (Abdollahi et al. 2013; Bayati et al. 2014; Pereira et al. 2014). These results are promising and may potentially lead to replacement of the plastic layer in food and liquid packaging, making these products more environmentally friendly. Meng and Manas-Zloczower (2015) studied the conductive properties of CNC/CNT (carbon nanotubes) composite films and found that the surface electrical resistivity of the films could be varied between 102 and 1011 Ω/sq by varying the CNT weight fraction, depending on end use. Similarly, films composed of CNC and graphene oxide exhibited improved conductivities (Valentini et al. 2013). These conductive films are potentially useful as electrodes for batteries, super capacitors, solar cells, and other flexible electronic devices. Another interesting application for CNCs is in the

pharmaceutical industry. It has been demonstrated that CNCs could be utilized as drug delivery excipients to facilitate the controlled release of drugs (Carlsson et al. 2013; Jackson et al. 2011; Plackett et al. 2014). The list of applications based on CNC containing films and coatings continues to grow across various disciplines ranging from food packaging, flexible electronics and energy storage, photonics, pharmacy, biomedical sciences, and tissue engineering (Abitbol et al. 2016; Hamad 2017; Hubbe et al. 2017).

Most of the applications demonstrated in the literature are produced using laboratory scale batch processes such as solvent casting, layer-by-layer deposition, filtration, and draw-down coating, often followed by slow drying at ambient conditions or in an oven. In order to make these applications commercially viable, it is important to understand the requirements that enable efficient fabrication techniques. Research groups have demonstrated applications using extrusion coating (Ambrosio-Martín et al. 2015; Fortunati et al. 2014) and foam coating (Kinnunen-Raudaskoski et al. 2014). Although both these methods are continuous processes, they have certain limitations. Extrusion coating is suitable with CNC as filler in a polymer matrix and is not practical as the concentration of CNC increases. Foam coating requires creation of a stable foam with air content approaching 90% (Kinnunen-Raudaskoski et al. 2014) and adds additional process steps. Roll-to-roll coating of CNFs on a paper-based substrate has been demonstrated by Kumar et al. (2016a). The role of CNF type, suspension rheology, and substrate properties on the coating process were also studied (Kumar et al. 2016b, 2017a, 2017b; Kumar 2018). Chowdhury et al. (2018) recently demonstrated roll-to-roll coating of CNC suspensions on a flexible plastic (polyethylene terephthalate) substrate using reverse-gravure metering. The maximum coating line speed achieved was 1.2 m/min but the main drawback of the reverse-gravure process is that coating thickness is inversely proportional to the line speed. To the best of our knowledge, continuous, roll-to-roll coating of CNC suspension as a thick layer on a paper-based substrate at speeds higher than 1.2 m/min is yet to be reported in the literature.

CNCs, owing to their high degree of crystallinity and relatively high viscosity even at low solids, pose certain challenges for roll-to-roll high-throughput processes. For example, the CNC films are brittle because of their high crystallinity and strong intramolecular hydrogen bonds. The latter can also cause inadequate adhesion to various substrates. The high water content of CNC suspensions presents its own challenges for continuous drying of the relatively thick wet coated layers. The objective of this work was to address these challenges by providing an understanding of the processability of CNC suspensions in a continuous process onto paperboard and to characterize the resulting coating quality in terms of surface, barrier, and substrate adhesion properties.

Experimental section

Materials

CNCs were obtained from Melodea Ltd. as a 3 wt% aqueous suspension at pH 4. Dissolving pulp was used as the source for CNCs, and sulfuric acid for the hydrolysis step. Figure 1 shows TEM images of the cellulose nanocrystals. Stability was assessed by zeta potential (0.1 wt%, 10 mM NaCl) and dynamic light scattering measurements (0.01 wt%, 10 mM NaCl). The zeta potential of the CNCs was approximately $-$ 40 mV, and the z-average dynamic light scattering size was 132 nm (Polydispersity index < 0.3). Sorbitol (D-sorbitol, 99%, Sigma-Aldrich) was used as a plasticizer to reduce the brittleness of the coatings (refer to supporting information). A commercial pigment coated paperboard, Trayforma^{TM} Special (Stora Enso) was used as a substrate for all the coatings in this work. The basis weight and thickness of the paperboard were 204 ± 2 g/m^2 and 270 ± 2 µm, respectively. This paperboard is referred to as "baseboard". Pigment coated board was chosen as the base substrate because of its higher surface smoothness and lower pore size compared to an uncoated board, which would result in improved coverage and retention of the CNC coating on the surface.

The baseboard was initially pre-coated with different primers (see Table 1) in order to improve the adhesion of CNC coatings to the baseboard. The choice of primers was based on our previous experience of coating micro-fibrillated cellulose on paperboard (Kumar et al. 2017a, b). A benchtop metered rod coater (K202 control coater, RK print-coat instruments Ltd.) was used to coat the primers onto the

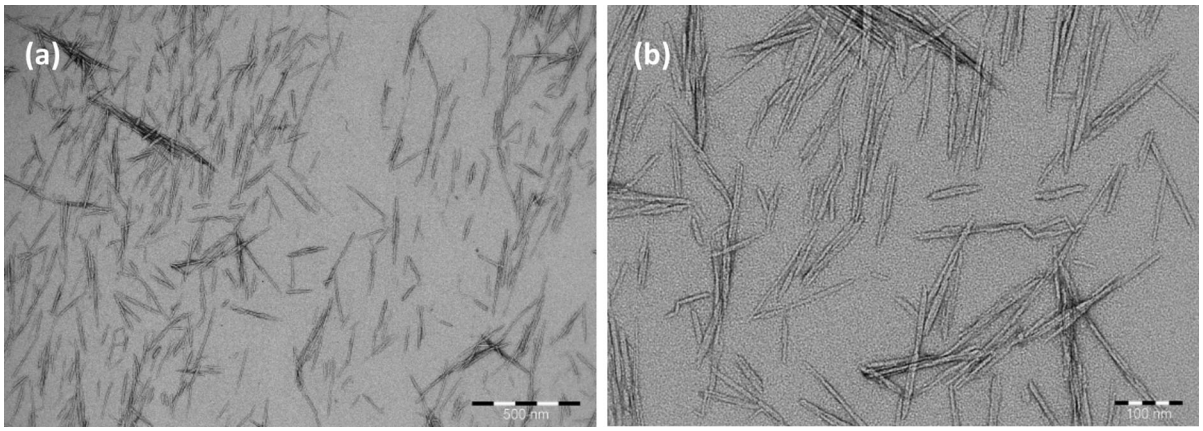

Fig. 1 TEM images of CNCs, **a** low resolution—scale bar: 500 nm and **b** high resolution—scale bar: 100 nm

Table 1 Primers used for pre-coating baseboard

Primer	Description	Supplier
FINNFIX® 10	Carboxymethyl cellulose (CMC), 5% solids	CP Kelco Oy
Omyajet 5010FL	Cationically dispersed $CaCO_3$ + 5 parts per hundred (pph) CMC + 5 pph latex binder, 30% solids	Omya International AG
Superfloc C-592	PolyDADMAC (Polydiallyldimethylammonium chloride—cationic polymer), 1% solids	Kemira Oyj
Raisimyl® 135	Cationic starch, 0.3% solids	Chemigate Oy

baseboard at wet thicknesses of 25 μm. A 3 wt% CNC suspension was applied at 500 μm wet thickness on these primer-coated baseboards using the same bench-top coater. A tape test (Standard: IPC-TM-650) was used as a qualitative measure of coating adhesion. Additional characterization of the primer coatings was done by measuring their air permeability (ABB Lorentzen & Wettre) and time-dependent water contact angles (CAM 200, KSV NIMA, Biolin Scientific Oy). Based on the findings from the above measurements (discussed below), cationic starch was chosen as the main primer for roll-to-roll coating of CNC suspensions.

Rheology

Rheology measurements of the CNC suspensions, both with and without sorbitol were carried out using a Paar Physica MCR300 rheometer (Anton Paar GmbH). A Couette geometry (radii of bob and cup are 13.3 and 14.5 mm respectively, vertical gap between bob and cup was kept at 5.7 mm) was used and all the measurements were done according to the standards specified in DIN 53019-1. Shear flow measurements were performed with a shear rate ramp of 0.1–1000 s^{-1} with 20 s per data point. Thixotropic behavior was measured by shearing the sample at 0.1 s^{-1} for 600 s, then at 1000 s^{-1} for 30 s and finally at 0.1 s^{-1} for 300 s. All samples were pre-sheared at 100 s^{-1} for 60 s and then left to equilibrate for 120 s before starting the measurements.

Roll-to-roll coating process

The baseboard was first pre-coated with a 0.3 wt% cationic starch solution using a Rotary Koater (RK PrintCoat Instruments Ltd.), which is a laboratory scale roll-to-roll pilot coating machine with operating speeds between 1 and 50 m/min, and depending on the requirement, it can be fitted with various coating/printing heads. It was equipped with a 5 kW infrared drying unit and two 10 kW hot-air dryers with adjustable airflows and temperatures reaching 200 °C. The starch solution was applied using a

reverse gravure coating unit. The gravure roll has a surface volume of 78.5 cm^3/m^2 (70 lpi × 127 μm) and applies a wet thickness of 16–25 μm (transfer fraction of 0.32). It is difficult to accurately determine the dry thickness of the starch layer applied to the baseboard due to the low solids content of the starch solution. Therefore, we assumed that the dry weight of the starch coating was less than 1 g/m^2. This starch-coated baseboard was subsequently coated with CNC suspensions using the same Rotary Koater but with a few modifications done in-house to coat nanocellulose suspensions. The setup is similar to the one used to coat micro-fibrillated cellulose by Kumar et al. (2017a, b). Analogous to micro/nano-fibrillated cellulose suspensions, CNC suspensions also have high viscosity and yield stress at low solids content and exhibit highly shear-thinning behavior (Kumar et al. 2016a, b; Nazari et al. 2016; Shafiei-Sabet et al. 2012). High shear rates can be achieved in a pressure driven flow when the suspension is passed through a narrow slot, causing a reduction in its apparent viscosity. The low viscosity suspension thus exiting the slot can then be transferred immediately to the substrate to form a uniform film. CNC suspension was fed into a custom-built slot-die (length 34 mm, width 74 mm, slot gap 500 μm, and distribution channel diameter 16 mm) from an air-pressurized feed vessel. The slot-die was installed at a 3 o'clock position relative to a backing roll and was used as both coating applicator and metering device. Figure 2 shows the schematic of the roll-to-roll coating setup, the positioning of the slot-die applicator, and an inside view of the slot-die. The pressure drop in the slot was controlled by adjusting the air pressure to the feed vessel. The wet coating thickness was controlled by precisely adjusting the gap between the substrate and the slot lips, and the excess coating was metered off and collected into the tray below. Four additional infrared dryers (2 kW each) and four hot air dryers (2 kW each) were installed on the machine to help with the drying process. Two different CNC suspensions, one with sorbitol (3.8 wt% CNC + 20 pph (parts per hundred, with respect to dry CNC) sorbitol) as plasticizer and the other without sorbitol (3 wt% CNC) were coated at different wet thicknesses and the coatings thus produced were characterized after conditioning them at 23 °C and 50% RH for at least 24 h.

Characterization of CNC coated samples

Cross section images of the coatings were obtained using a Scanning Electron Microscope (SEM) (Q250 FEG, FEI). These images were used to determine the corresponding coating thicknesses. Due to the baseboard's variation in basis weight compared to the CNC coatings, traditional gravimetric methods do not give accurate values for the coat weights. Therefore, they were calculated from the coating thicknesses acquired through SEM. The density of CNCs was taken as 1.55 g/cm^3 (Dufresne 2013).

Surface roughness of the coatings were measured using Parker Print-Surf (PPS) smoothness tester (PPS ME-90, Messmer Büchel BV). Average roughness of five parallel measurements is reported in micrometers (μm). A stylus profilometer (DektakXT®, Bruker) was also used to measure the surface roughness of the coatings. The measurement area was 1 × 1 mm^2 and the corresponding average roughness (R_a) is reported in micrometers. PPS and stylus profilometer differ in their measurement technique. The former measures the air leak rate from the surface against a rubber backing to simulate the conditions experienced during printing processes; while the latter measures the average deflection of a stylus moving along the surface. Stylus profilometer is similar to AFM (Atomic Force Microscopy) measurement technique except, the length scales are larger. AFM roughness (MultiMode, Bruker, PeakForce Tapping mode) was also measured for the coatings and the average value at 500 nm length scales is reported. Air permeability of the coatings is reported in μm/Pa s as average value of five measurements.

Adhesion of the CNC coating layer to the baseboard was quantified by measuring the force required to peel off the coating from the baseboard using an IMASS SP-2000 peel tester. A tape (TZe-C51, Brother UK Ltd.) was attached to the surface of the substrate at one edge while the opposite edge was attached to a clamp, which in turn was attached to a 2 kg load cell. The tape was pulled over a length of 33 mm at a speed of 54 mm/s and the force required to peel the tape was measured by the load cell. The average force value of five measurements is reported.

Water vapor transmission rate (WVTR) was measured for the coated samples according to the ASTM standard, E96/E96 M-05. The desiccant method was used for the tests where a fixed amount of anhydrous

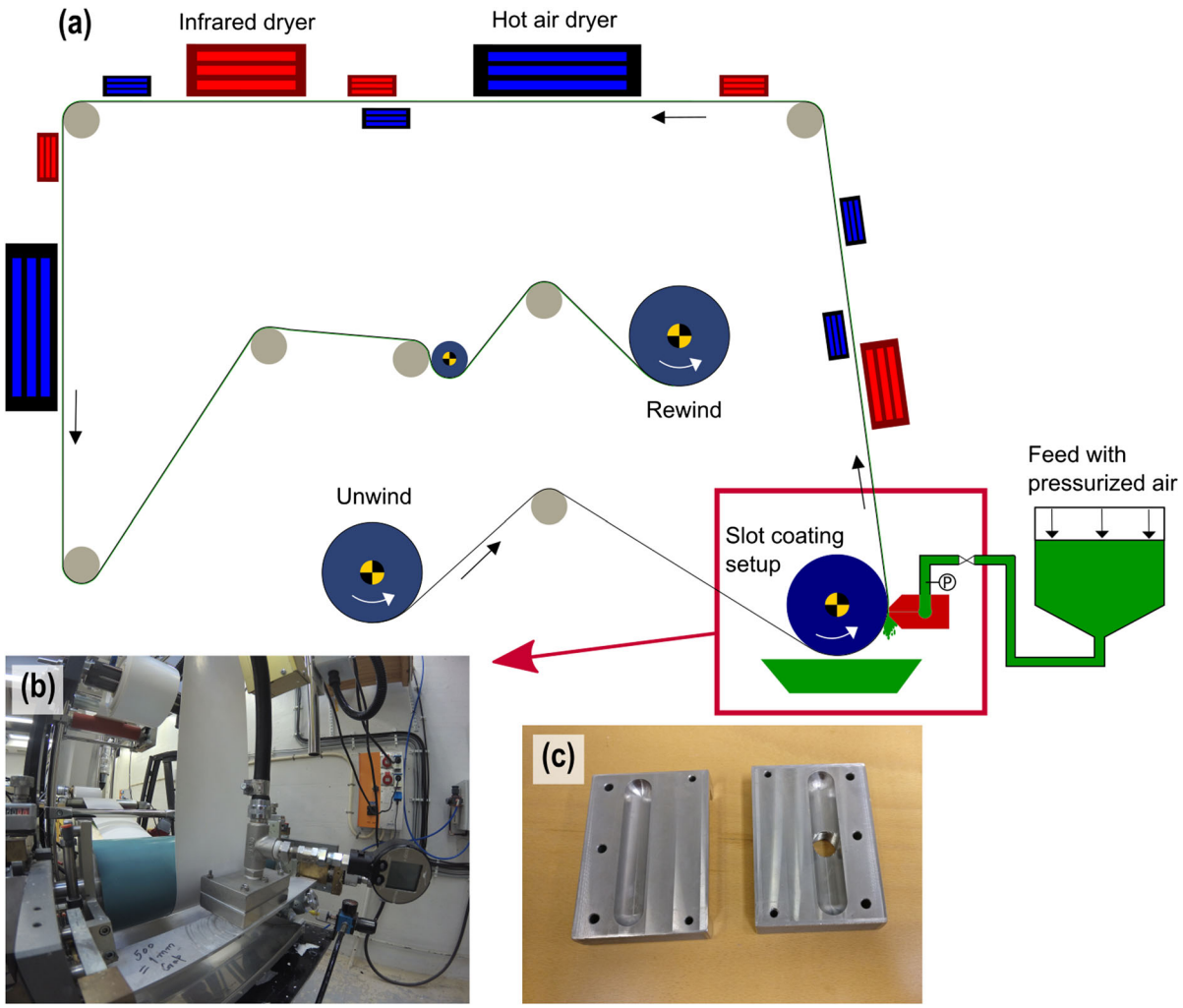

Fig. 2 **a** Schematic of the roll-to-roll coating setup; **b** positioning of the slot die applicator; **c** inside view of the slot die

$CaCl_2$ (Honeywell FlukaTM) was placed in a dish covered with the test specimen and the edges sealed with molten wax. This assembly was placed in a climate-controlled chamber (23 °C, 50% RH) for 24 h. Water vapor transmission rate (WVTR) through the specimen into the desiccant was calculated by measuring the increase in the weight of the cup over the duration of the experiment. The average value of three parallel measurements is reported in g/m^2 day. A similar method was used to determine heptane vapor transmission rate (HVTR) (Miettinen et al. 2015). In this method, the salt was replaced with 10–15 ml of n-heptane (Sigma Aldrich) and test cups with rubber gaskets and screwable tops were used to get a better seal. A sponge was placed inside the cup in order to achieve rapid liquid/gas saturation. The entire assembly was again placed in a climate-controlled chamber (23 °C, 50% RH) for 24 h and the reduction of weight due to evaporation of heptane through the sample was used to calculate HVTR. The average value of three measurements is reported in g/m^2 day.

Results and discussion

Rheology

Rheology of the CNC suspensions plays an important role in the coating process. Similar to micro- and nano-fibrillated cellulose suspensions, CNC suspensions

used in this work (see Fig. 3a) also exhibit very high viscosity and yield stress at a low solids content of just 3%, and are highly shear thinning. This shear-thinning behavior is in fact utilized in the slot coating process to coat a uniform CNC film onto the substrate. When the CNC suspension is passed through a narrow slot, its shear rate increases and the corresponding viscosity drops. The resulting low viscosity suspension is transferred immediately to the substrate and applied as a uniform wet-film. Compared to traditional coating processes such as blade or rod coating, slot coating has the advantage that the shear rate is independent of line speed. Desired shear rates can be achieved by adjusting the pressure drop across the slot gap and its dimensions, which in turn change the corresponding flow rate. The excess flow is metered off by the slot's top lip. As the suspension exits the slot lip, there is a sudden drop in shear rate and it takes a certain time for the suspension to recover its viscosity. The recovery rate depends on a number of factors such as, total solids content of the suspension, plasticizer type and amount, and difference in the shear rates before and after leaving the slot lip. In order to form a uniform film on the substrate, the suspension should stay fluidized (low viscosity region) while it is being applied onto the surface, i.e., the time spent by the suspension after it exits the slot and while being metered by the slot's top lip. Figure 3b shows the time dependent viscosity behavior of the CNC suspensions at different solids concentrations, when the shear rate was increased from 0.1 to 1000 s^{-1} and then reduced to 0.1 s^{-1}. Viscosity vs. shear rates for these suspensions are also shown in Fig. 3.

It is seen from the above figure that sorbitol does not play a major role in the rheological behavior of the suspensions, probably due to its low molecular weight. The rheology of the suspension, is therefore, largely controlled by the concentration of CNC. The power law index for all of the suspensions is approximately 0.2, thus confirming their high shear thinning behavior. With increasing CNC concentration, the viscosity recovers faster as the shear rate goes from high to low. Table 2 shows the time taken by each suspension to regain to 50, 75 and 100% of their corresponding maximum viscosities when the shear rate goes down from 1000 to 0.1 s^{-1}.

The shear rates in the slot used herein are typically between 10,000 and 60,000 s^{-1} depending on the pressure drop and flow rate. The shear rates between the slot lip and the substrate during metering are between 100 and 3200 s^{-1} depending on the line speed and the gap between the slot and the substrate (called slot-web gap—SWG). The time the suspension spends being metered after exiting the slot is a function of line speed. For example, at a SWG of 400 μm and a line speed of 2.5 m/min, the metering time is about 0.12 s and the corresponding shear rate is 105 s^{-1}. Similarly, at a SWG of 50 μm and a line speed of 10 m/min, the metering time is 0.03 s and the corresponding shear rate is 3200 s^{-1}. Therefore, by extrapolating the findings from Table 2, it is assumed that the suspension remains fluidized during metering, thus enabling uniform film formation.

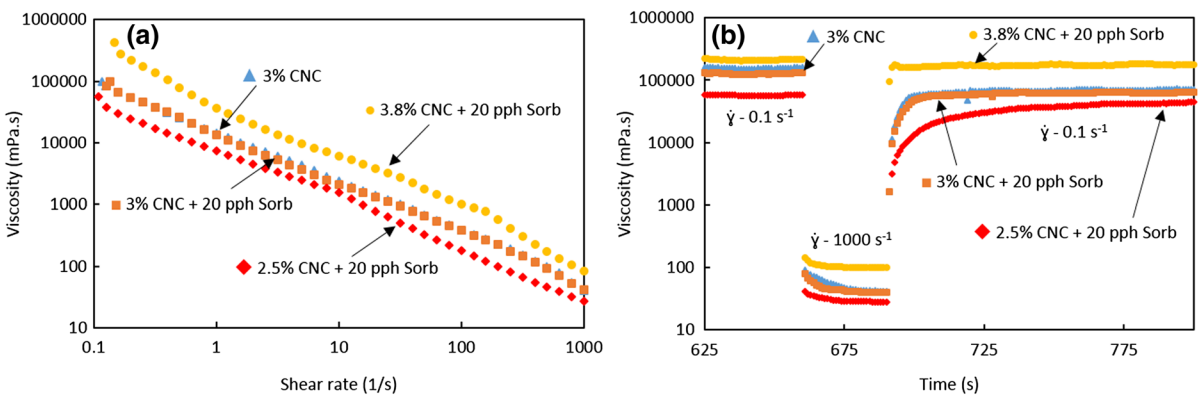

Fig. 3 **a** Viscosity versus shear rate for CNC suspensions at different solids concentration; **b** Thixotropic behavior for CNC suspensions when sheared at, 0.1 s^{-1} for 600 s, 1000 s^{-1} for 30 s and 0.1 s^{-1} for 300 s

Table 2 Time (t_R) in seconds required for CNC suspensions to recover 50, 75, and 100% of their corresponding maximum viscosities when the shear rate is decreased from 1000 to 0.1 s^{-1}

Suspension	t_R (50%)	t_R (75%)	t_R (100%)
3% CNC	5	7	31
3% CNC + 20 pph Sorb	6	10	42
2.5% CNC + 20 pph Sorb	18	38	82
3.8% CNC + 20 pph Sorb	N/A*	1	6

*Below the instrument's detection limit

Pre-coating

As the wet film dries on the surface of the baseboard, strong CNC-CNC interactions may result in poor adhesion to various substrates. Hydrophilic substrates, for example, the recycled fiber linerboard used by Kumar et al. (2016a, b) are an exception because of the cellulose-cellulose interactions between CNCs and the substrate. However, uncoated paperboards require a certain minimum coat weight to achieve full coverage. This can be as high as 5 g/m^2 depending on the substrate's surface roughness (Kumar et al. 2016a, b). Commercially produced coated paperboards on the other hand have typically poor adhesion to CNCs; however, they have relatively smoother surfaces and enable full coverage at low coat weights. Considering the high production costs of CNCs, it is desirable to utilize the least amount of material to reach the required target properties. Less coated material also translates to savings in drying costs. Therefore, several primers were explored to improve the adhesion of CNCs to the baseboard (pigment-coated paperboard).

All the four primers: CMC, $CaCO_3$, polyDADMAC and cationic starch, when coated on the baseboard, reduced its water contact angle (see Table 3). $CaCO_3$ pre-coating resulted in the lowest water contact angle because in addition to providing a more hydrophilic surface, it also created a porous structure that facilitates the spreading of the water droplet on the surface. Baseboards coated with CMC and polyDADMAC reached similar contact angle values after 1 s of spreading and cationic starch coated board showed the highest contact angles of the primers. This might be due to the low solids content of the cationic starch solution (0.3%) and the resulting lower dry coat weight, potentially providing incomplete coverage. CNC suspension spreads uniformly on all the pre-coated baseboards due to their lowered contact angles. Tape tests were performed to assess the adhesion of CNC coatings to the pre-coated baseboards (see supporting information). For $CaCO_3$ coated baseboard, the failure was at the interface between the baseboard and the primer coating, indicating poor adhesion between the two. The CNC coating was easy to peel off for polyDADMAC-coated baseboard. Although, few pigment particles from the baseboard were visible, the tape required considerably lower force to peel off and since polyDADMAC forms a transparent layer, it was difficult to verify where the failure occurred. CNC coatings showed strong adhesion to CMC and starch coated baseboards. In both these cases, either the failure was at the baseboard's pigment coated layer or there was no failure at all, in which case the tape came off clean with CNC coating still intact on the baseboard. This indicates that CNCs form strong bonds with CMC and cationic starch, which in turn adhere strongly to the baseboard. The cationic charge in the starch coating might be playing a major role in improving the adhesion of the anionic CNCs. Similar experiments with anionic starch were performed and they resulted in poor adhesion of CNCs to the substrate. Cationic starch was preferred as a primer for roll-to-roll coatings because it provided higher air permeability (Table 3) compared to CMC coated baseboard. Higher air permeability indicates a more open structure, which aids in faster drying of the

Table 3 Air permeability and contact angles for different pre-coated baseboards

	Air permeability (μm/Pa s)	Contact angle (°) evolution in time		
		0.1 s	0.5 s	1 s
Baseboard	$9 \times 10^{-3} \pm 0.7 \times 10^{-3}$	86 ± 3	78 ± 2	72 ± 1
CMC	N/A*	33 ± 3	32 ± 3	32 ± 3
$CaCO_3$	$17 \times 10^{-3} \pm 0.4 \times 10^{-3}$	33 ± 1	22 ± 1	20 ± 1
PolyDADMAC	$24 \times 10^{-3} \pm 1.2 \times 10^{-3}$	52 ± 1	34 ± 2	29 ± 1
Cationic starch	$16 \times 10^{-3} \pm 0.9 \times 10^{-3}$	64 ± 3	61 ± 1	58 ± 1

*N/A not analyzed, below the instrument's detection limit

CNC coatings. The fact that pre-coated baseboard had higher air permeability than the baseboard, suggests fiber swelling of the baseboard during the pre-coating.

Characterization of CNC coated board

CNC suspensions, with and without sorbitol, were coated on the pre-coated (cationic starch) baseboard using the roll-to-roll slot coating process. CNC coatings with several different coat weights were produced and characterized for their coating uniformity, adhesion, and barrier properties. Two CNC suspensions were used for the coatings, one was a 3 wt% CNC suspension without sorbitol and the other a 3.8 wt% CNC suspension with 20 pph sorbitol. Coat weights of the applied CNC suspension were varied by changing the SWG, which is set by moving the slot perpendicular to the backing roll's axis of rotation and a gauge is used for the fine adjustment. The actual thickness of the wet coating applied is lower than the SWG due to factors such as, swelling of the substrate, slot die geometry and position (Ding et al. 2016). Table 4 lists the thicknesses of the dry CNC coatings obtained from SEM cross-section images, their corresponding line speeds, and calculated coat weights and wet film thicknesses. Since the drying capacity on the coater is limited, line speeds for each coat weight were adjusted to enable continuous coating and drying. Higher coat weights demand larger drying capacity, hence the lower line speed and vice versa.

The coating thicknesses vary from 0.9 to 7.2 μm and their corresponding coat weights range from 1.4 to 11 g/m^2 respectively. Higher coat weights were not possible due to limitations in the machine's drying capacity but can be achieved either by using suspensions with higher solids content or by multi-layer coatings. The current setup for slot die coating is limited to a minimum wet thickness of 15 μm due to practical restrictions in accurately setting the SWG (Ding et al. 2016). Therefore, coatings lower than 1.4 g/m^2 (20 μm wet thickness) were not possible with the CNC concentrations that were used. Coat weights measured by gravimetric method are also reported in Table 4. They show higher values and larger variations compared to the coat weights calculated from SEM thicknesses and they do not follow any clear trend in relation to the set SWG. This could be attributed to the baseboard's variation in basis weight on the measurements. Therefore, coat weights determined through SEM cross-sections were used for the rest of the work. SEM cross-section images (see Fig. 4) and AFM surface images (see Fig. 5) indicate full and uniform coverage of CNC coatings on the baseboard. Both the coatings with and without sorbitol look similar in the cross-section images.

The surface roughness values from both PPS and stylus profilometer show an increasing trend with increasing coat weights (see Table 5). Calendering reduces the roughness of the coatings to the same value, thus, the increase in the roughness can be attributed to swelling of fibers in the baseboard. Higher coat weights apply larger amounts of water, which results in increased fiber swelling and thus, a roughness increase. Differences between the roughness values for PPS and stylus profilometer are due to their different measurement techniques but with a

Table 4 Coating line speeds, thicknesses, coat weights and wet film thicknesses for the different CNC coatings

	Line speed (m/min)	Coating thickness (μm)—SEM	Coat weight (g/m^2)—SEM*	Coat weight (g/m^2)—gravimetric	Wet film thickness (μm)*
3 wt% CNC	3	4.9 ± 0.1	7.6 ± 0.1	13.3 ± 3.3	160
	3	2.8 ± 0.1	4.3 ± 0.2	7.9 ± 0.8	90
	4	2.1 ± 0.1	3.3 ± 0.2	6.1 ± 1.4	70
3.8 wt% CNC + 20 pph sorbitol	2.5	7.2 ± 0.7	11.2 ± 1.1	9.7 ± 1.2	200
	3	4.3 ± 0.4	6.7 ± 0.6	2.0 ± 0.9	120
	4	2.3 ± 0.1	3.5 ± 0.2	6.1 ± 0.7	50
	4	0.9 ± 0.1	1.4 ± 0.1	1.7 ± 0.5	20
	10	1.3 ± 0.1	2.0 ± 0.2	6.2 ± 0.5	30

*Calculated from thickness obtained through SEM

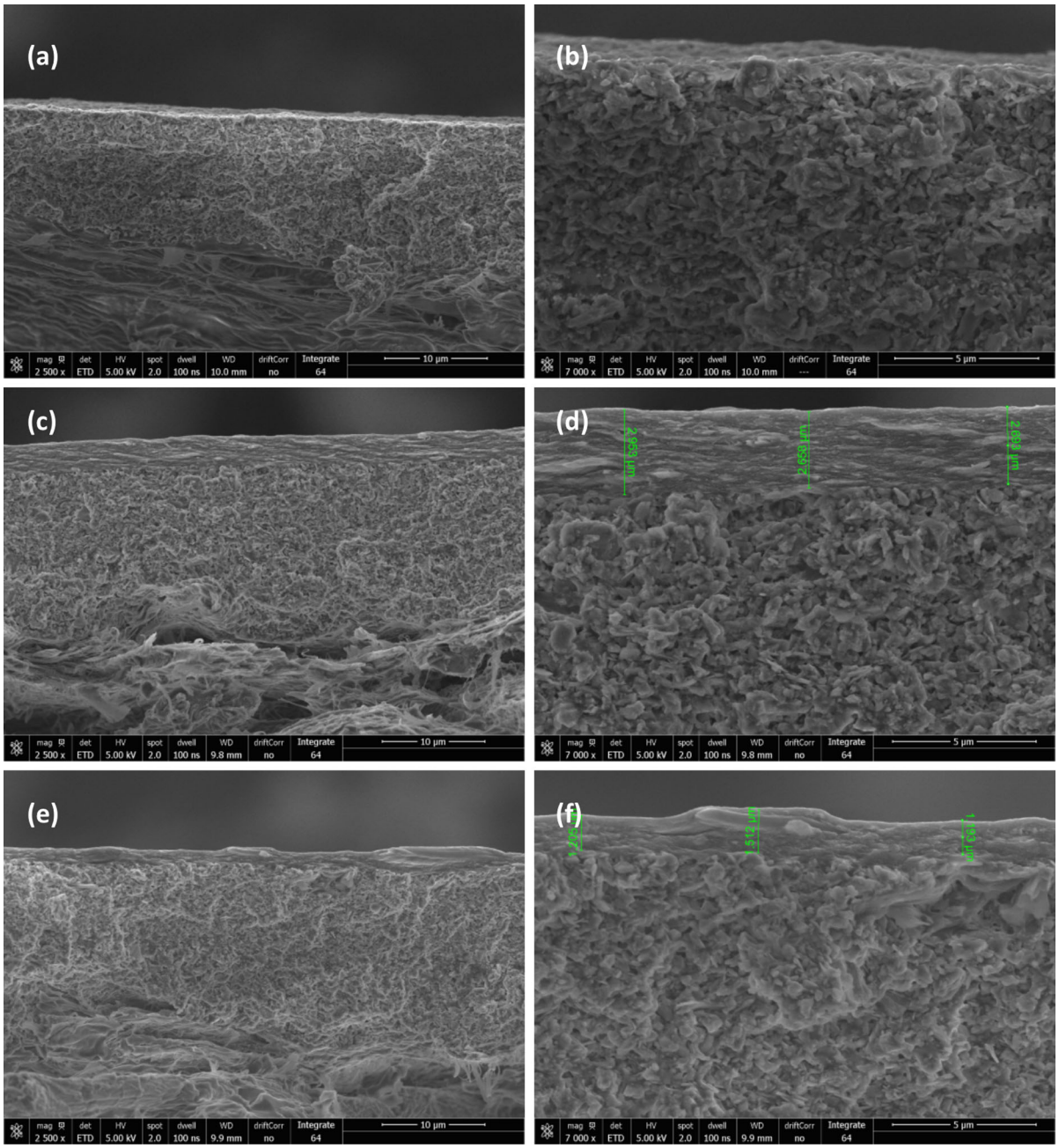

Fig. 4 SEM cross-sections. **a**, **b** Baseboard; **c**, **d** 3 wt% CNC coating (4.3 g/m^2); **e**, **f** 3.8 wt% CNC + 20 pph sorbitol coating (2 g/m^2)

reasonable agreement in between. While both PPS and stylus profilometer values are influenced heavily by the baseboard's roughness, the AFM roughness on the other hand is measured at smaller length scales (500 nm) and is not influenced by the baseboard's large-scale roughness. All the CNC coatings showed similar AFM roughness values of approximately 4 nm (see Table 5), which is smaller than the width of the CNCs, therefore, indicating uniform distribution of the CNCs without large aggregates. CNC coatings, in general, have been reported to show reduced air permeabilities due to their ability to form a closed

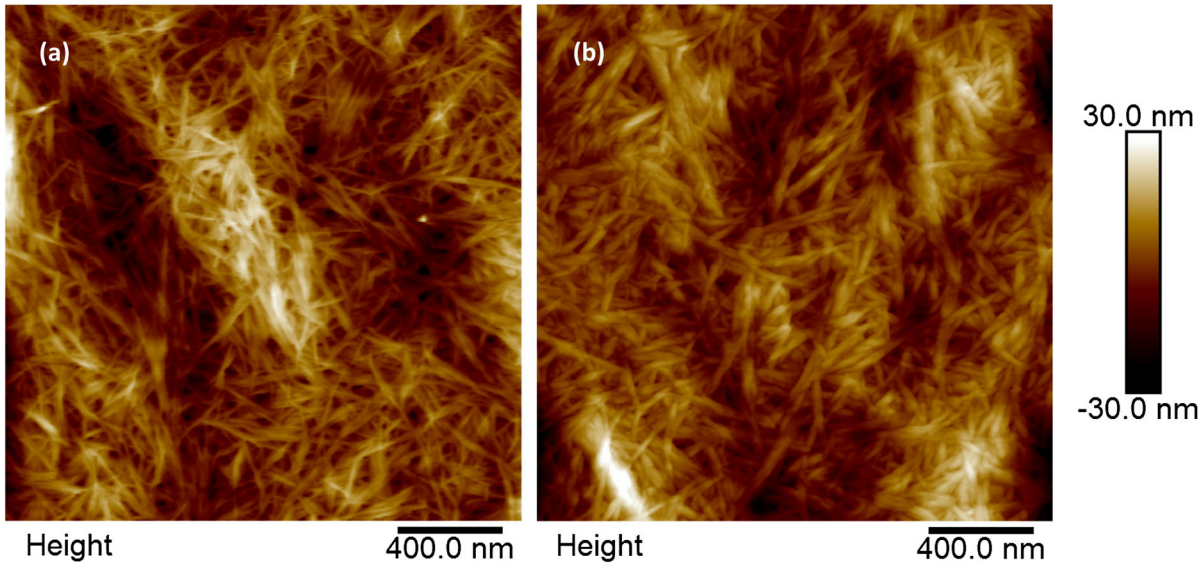

Fig. 5 AFM surface images. **a** 3.8 wt% CNC + 20 pph sorbitol coating (2 g/m^2); **b** 3 wt% CNC coating (3.3 g/m^2)

Table 5 Roughness values from PPS, stylus profilometer and AFM topography

	Coat weight (g/m^2)	PPS roughness (μm)	Stylus profilometer—R_a (μm)	AFM roughness (nm)
Base board	–	1.50 ± 0.03	1.22	–
3 wt% CNC	7.6	3.46 ± 0.15	1.71	3.1 ± 0.2
	4.3	3.22 ± 0.04	1.47	5.6 ± 3.8
	3.3	3.04 ± 0.06	1.56	3.8 ± 0.4
3.8 wt% CNC+20 pph sorbitol	11.2	4.03 ± 0.07	2.2	4.0 ± 0.3
	6.7	3.32 ± 0.15	1.34	3.6 ± 0.5
	3.5	2.90 ± 0.08	1.23	3.7 ± 0.5
	2.0	2.55 ± 0.09	0.96	4.4 ± 0.5
	1.4	2.42 ± 0.04	0.96	4.9 ± 1.4

network structure (Gicquel et al. 2017). The air permeabilities for all the coatings produced herein fall below the instrument's detection limit, thus, indicating full coating coverage. Such low values for air permeability for a CNC coated paperboard at coat weights as low as 1.4 g/m^2, have not been reported in the literature before. Pigment coated boards in general have very low air permeabilities and the use of such a substrate as a base for CNC coatings certainly plays a role with the improved performance.

Adhesion of the CNC coating layer to the baseboard was quantified by measuring the force required to peel off the coating from the baseboard. As the tape is peeled off at a constant speed, a load cell measures the corresponding force and plots it as function of time. There is an initial peak in the force when the coating layer fails and starts coming off with the tape after which the force plateaus at a lower value as the failed interface is peeled off (see Supporting Information for an example of force vs. time curve). Therefore, the maximum and the average force values can be utilized to quantify the adhesion strength of the coatings. The maximum force is similar for all the coatings and is identical to the maximum force required to cause failure between the pigment-coating layer and the baseboard (see Table 6). This indicates that all the CNC layers adhere to the pigment-coating layer as strongly as the pigment-coating layer adheres to the fibers in the baseboard. Examining the failed surface and its corresponding peeled tape (see Supporting

Table 6 Peel test force values for the CNC coatings

	Coat weight (g/m^2)	Max force (N)	Average force (N)
Baseboard	–	6.6 ± 0.8	5.3 ± 2.5
3 wt% CNC	7.6	6.4 ± 1.4	2.5 ± 1.6
	4.3	7.4 ± 1.9	4.4 ± 3.6
	3.3	8.0 ± 1.5	6.2 ± 0.8
3.8 wt% CNC + 20 pph sorbitol	11.2	8.0 ± 0.6	6.4 ± 1.0
	6.7	8.3 ± 0.5	6.3 ± 0.8
	3.5	7.9 ± 0.7	5.6 ± 1.6
	2.0	8.2 ± 2.0	6.0 ± 1.8
	1.4	7.0 ± 2.0	5.9 ± 1.4

Table 7 Barrier properties for heptane (HVTR) and water vapor (WVTR) for the CNC coatings

	Coat weight (g/m^2)	HVTR (g/m^2 day)	WVTR (g/m^2 day)
Base board		1710 ± 78	174 ± 5
3 wt% CNC	7.6	24 ± 9	138 ± 17
	4.3	13 ± 4	148 ± 20
	3.3	127 ± 24	146 ± 33
3.8 wt% CNC + 20 pph sorbitol	11.2	29 ± 16	41 ± 3
	6.7	18 ± 11	59 ± 3
	3.5	21 ± 13	85 ± 4
	2.0	187 ± 38	90 ± 2
	1.4	131 ± 35	89 ± 8

Information) showed pigment-coating and CNC-coating fragments on both the surfaces thus, suggesting that the failure is a combination of adhesive (interface between CNC coating and baseboard) and cohesive (within pigment-coating layer and CNC-coating layer) failures. The average force indicates the force required to peel the already failed layer, hence, its lower value compared to the corresponding maximum force. It is seen from Table 6 that the average force for CNC coatings without sorbitol reduced as the coat weight increased, while the average force for CNC coatings containing sorbitol remained the same irrespective of the coat weights studied, and that it is close to the baseboard's value. This indicates that in addition to cationic starch, sorbitol also plays a role in improving CNC coating's adhesion to the baseboard. Sorbitol has all the hydroxyl groups easily accessible to potentially interact with both cellulose nanocrystals and starch, thus, further improving adhesion. CNC coatings without sorbitol lack this added advantage and as the coat weight increases, cationic starch is not sufficient to create resistance to the peeling force.

Majority of the applications based on CNCs require barrier against a variety of liquids and gases depending on the end use application. Therefore, the CNC coatings were further characterized for their barrier against mineral oil and water vapor. Heptane vapor transmission rate (HVTR) can be a reliable indicator for barrier against mineral oils because heptane is a relatively small molecule compared to mineral oil components. If the coatings provide barrier against heptane they would certainly provide barrier against larger molecular weight oil components. It is seen from Table 7 that HVTR values for CNC coatings are significantly reduced compared to those for baseboard. All the coatings show a reduction of over 90% and for coat weights above 3.5 g/m^2, the reduction is almost 99%. HVTR values are sensitive to coating defects in the sample, hence, the reason for the higher standard deviation. Therefore, it is difficult to make comparisons between various coat weights especially when differences in HVTR are not large. CNC coatings containing sorbitol reduced the water vapor transmission rate (WVTR) by more than 50% while those without sorbitol did not have considerable impact (see

Table 7). These findings are similar to results reported in other, but related, systems (Herrera et al. 2017). The small molecular weight of sorbitol together with its abundance of hydroxyl groups forms strong hydrogen bonds with cellulose nanocrystals thus, creating a stronger and more closed coating structure. This slows down the movement of water molecules resulting in lower WVTR values. However, it has to be kept in mind that WVTRs typically increase sharply as the relative humidity increases and the barrier is not sufficient for applications where there is contact with liquid water. CNC based films and coatings have also been reported to provide barrier against oxygen (Li et al. 2013) and grease (Gicquel et al. 2017). Although these measurements have not been performed on the CNC coatings produced in this work, they can be expected to give promising results and this could be the focus for future work on CNC based coatings.

Conclusions

High-throughput roll-to-roll coating of CNC suspensions on paperboard was successfully demonstrated for the first time, and coating speeds as high as 10 m/min have been achieved. Various challenges related to processing of CNC suspensions into coatings, such as high viscosity and yield stress at low solids content, brittleness of CNC films and poor adhesion of CNC coatings to commercial paperboard were addressed. Rheological properties of CNC suspensions at different solids concentrations were studied and their inherent shear-thinning behavior was utilized by passing them through a narrow slot gap. The low viscosity suspension thus exiting the slot was applied as a uniform coating onto paperboard. Using a smooth substrate, such as a commercial pigment-coated paperboard ensured full coverage and high peel adhesion forces even at coat weights as low as 1.4 g/m^2 and resulted in smoother coatings. Adhesion of CNC coatings to the pigment-coated paperboard was improved by applying a thin layer (less than 1 g/m^2) of cationic starch as primer coating. SEM cross-sections showed uniform CNC coatings with thicknesses ranging from 0.9 to 7 μm and their corresponding calculated coat weights varying from 1.4 to 11 g/m^2. Adding sorbitol as a plasticizer made CNC coatings flexible and less brittle, and had a positive impact on adhesion and barrier properties of the resulting coatings. There was a significant reduction in heptane vapor and water vapor transmission rates. For coat weights above 3.5 g/m^2, HVTR values were reduced by up to 99% and WVTRs by up to 75%.

Acknowledgments We thank Stora Enso, Omya International, CP Kelco and; Chemigate for kindly providing us with pigment-coated paperboard, $CaCO_3$ pigment, CMC and cationic starch respectively. The project was partly funded by VINNOVA testbed project called TinyBTalented. TA acknowledges Marie Skłodowska-Curie actions as research fellow and AS the Nils and Dorthi Troëdsson Foundation for Scientific Research.

References

Abdollahi M, Alboofetileh M, Behrooz R, Rezaei M, Miraki R (2013) Reducing water sensitivity of alginate bio-nanocomposite film using cellulose nanoparticles. Int J Biol Macromol 54:166–173. https://doi.org/10.1016/j.ijbiomac.2012.12.016

Abitbol T, Rivkin A, Cao Y, Nevo Y, Abraham E, Ben-Shalom T, Lapidot S, Shoseyov O (2016) Nanocellulose, a tiny fiber with huge applications. Curr Opin Biotechnol 39:76–88. https://doi.org/10.1016/j.copbio.2016.01.002

Ambrosio-Martín J, Fabra MJ, Lopez-Rubio A, Lagaron JM (2015) Melt polycondensation to improve the dispersion of bacterial cellulose into polylactide via melt compounding: enhanced barrier and mechanical properties. Cellulose 22:1201–1226. https://doi.org/10.1007/s10570-014-0523-9

Bayati F, Boluk Y, Choi P (2014) Diffusion behavior of water at infinite dilution in hydroxypropyl xylan films with sorbitol and cellulose nanocrystals. ACS Sustain Chem Eng 2:1305–1311. https://doi.org/10.1021/sc500133p

Brodin FW, Gregersen OW, Syverud K (2014) Cellulose nanofibrils: challenges and possibilities as a paper additive or coating material–a review. Nord Pulp Pap Res J 29:156–166. https://doi.org/10.3183/NPPRJ-2014-29-01-p156-166

Carlsson DO, Hua K, Forsgren J, Mihranyan A (2013) Aspirin degradation in surface-charged TEMPO-oxidized mesoporous crystalline nanocellulose. Int J Pharm 461:74

Chowdhury RA, Clarkson C, Youngblood J (2018) Continuous roll-to-roll fabrication of transparent cellulose nanocrystal (CNC) coatings with controlled anisotropy. Cellulose 25:1769–1781. https://doi.org/10.1007/s10570-018-1688-4

Ding X, Liu J, Harris TAL (2016) A review of the operating limits in slot die coating processes. AIChE J 62:2508–2524. https://doi.org/10.1002/aic.15268

Dufresne A (2013) Nanocellulose: a new ageless bionanomaterial. Mater Today 16:220–227. https://doi.org/10.1016/j.mattod.2013.06.004

Eichhorn SJ, Dufresne A, Aranguren MM, Capadona JR, Rowan SJ, Weder C, Thielemans W, Roman M, Renneckar S, Gindl W (2010) Review: current international research into

cellulose nanofibres and composites. J Mater Sci 45:1–33. https://doi.org/10.1007/s10853-009-3874-0

Elazzouzi-Hafraoui S, Nishiyama Y, Putaux J, Heux L, Dubreuil F, Rochas C (2007) The shape and size distribution of crystalline nanoparticles prepared by acid hydrolysis of native cellulose. Biomacromol 9:57–65. https://doi.org/10.1021/bm700769p

Feng X, Meng X, Zhao J, Miao M, Shi L, Zhang S, Fang J (2015) Extraction and preparation of cellulose nanocrystals from dealginate kelp residue: structures and morphological characterization. Cellulose 22:1763–1772. https://doi.org/10.1007/s10570-015-0617-z

Fortunati E, Peltzer M, Armentano I, Torre L, Jiménez A, Kenny JM (2012) Effects of modified cellulose nanocrystals on the barrier and migration properties of PLA nano-biocomposites. Carbohydr Polym 90:948–956. https://doi.org/10.1016/j.carbpol.2012.06.025

Fortunati E, Luzi F, Puglia D, Dominici F, Santulli C, Kenny JM, Torre L (2014) Investigation of thermo-mechanical, chemical and degradative properties of PLA-limonene films reinforced with cellulose nanocrystals extracted from *Phormium tenax* leaves. Eur Polym J 56:77–91. https://doi.org/10.1016/j.eurpolymj.2014.03.030

Gicquel E, Martin C, Garrido Yanez J, Bras J (2017) Cellulose nanocrystals as new bio-based coating layer for improving fiber-based mechanical and barrier properties. J Mater Sci 52:3048–3061. https://doi.org/10.1007/s10853-016-0589-x

Habibi Y, Lucia LA, Rojas OJ (2010) Cellulose nanocrystals: chemistry, self-assembly, and applications. Chem Rev 110:3479

Hamad WY (2017) Cellulose nanocrystals and nanofibrils in advanced applications. In: Kargarzadeh H, Ahmad I, Thomas S, Dufresne A (eds) Handbook of nanocellulose and cellulose nanocomposites. Wiley, Hoboken, pp 799–832

Herrera MA, Mathew AP, Oksman K (2017) Barrier and mechanical properties of plasticized and cross-linked nanocellulose coatings for paper packaging applications. Cellulose 24:3969–3980. https://doi.org/10.1007/s10570-017-1405-8

Hubbe MA, Ferrer A, Tyagi P, Yin Y, Salas C, Pal L, Rojas OJ (2017) Nanocellulose in thin films, coatings, and plies for packaging applications: a review. BioResources 12:2143–2233. https://doi.org/10.15376/biores.12.1.2143-2233

Isogai A (2013) Wood nanocelluloses: fundamentals and applications as new bio-based nanomaterials. J Wood Sci 59:449–459. https://doi.org/10.1007/s10086-013-1365-z

Jackson JK, Letchford K, Wasserman BZ, Ye L, Hamad WY, Burt HM (2011) The use of nanocrystalline cellulose for the binding and controlled release of drugs. Int J Nanomed 6:321–330. https://doi.org/10.2147/IJN.S16749

Kinnunen-Raudaskoski K, Hjelt T, Kenttä E, Forsström U (2014) Thin coatings for paper by foam coating. Tappi J 13:9–19

Klemm D, Kramer F, Moritz S, Lindström T, Ankerfors M, Gray D, Dorris A (2011) Nanocelluloses: a new family of nature-based materials. Angew Chem Int Ed 50:5438–5466. https://doi.org/10.1002/anie.201001273

Kumar V (2018) Roll-to-roll processing of nanocellulose into coatings, Åbo Akademi University

Kumar V, Elfving A, Koivula H, Bousfield D, Toivakka M (2016a) Roll-to-roll processed cellulose nanofiber coatings. Ind Eng Chem Res 55:3603–3613. https://doi.org/10.1021/acs.iecr.6b00417

Kumar V, Nazari B, Bousfield D, Toivakka M (2016b) Rheology of microfibrillated cellulose suspensions in pressure-driven flow. Appl Rheol 26:43534. https://doi.org/10.3933/APPLRHEOL-26-43534

Kumar V, Koppolu VR, Bousfield D, Toivakka M (2017a) Substrate role in coating of microfibrillated cellulose suspensions. Cellulose 24:1247–1260. https://doi.org/10.1007/s10570-017-1201-5

Kumar V, Ottesen V, Syverud K, Gregersen ØW, Toivakka M (2017b) Coatability of cellulose nanofibril suspensions: role of rheology and water retention. BioResources 12:7656–7679. https://doi.org/10.15376/biores.12.4.7656-7679

Lavoine N, Desloges I, Dufresne A, Bras J (2012) Microfibrillated cellulose–its barrier properties and applications in cellulosic materials: a review. Carbohydr Polym 90:735–764. https://doi.org/10.1016/j.carbpol.2012.05.026

Li F, Biagioni P, Bollani M, Maccagnan A, Piergiovanni L (2013) Multi-functional coating of cellulose nanocrystals for flexible packaging applications. Cellulose 20:2491–2504. https://doi.org/10.1007/s10570-013-0015-3

Lindström T, Naderi A, Wiberg A (2015) Large Scale applications of nanocellulosic materials. Palpu Chongi Gisul J Korea Tech Assoc Pulp Pap Ind 47:5–21. https://doi.org/10.7584/ktappi.2015.47.6.005

Mariano M, El Kissi N, Dufresne A (2014) Cellulose nanocrystals and related nanocomposites: review of some properties and challenges. J Polym Sci, Part B: Polym Phys 52:791–806. https://doi.org/10.1002/polb.23490

Meng Q, Manas-Zloczower I (2015) Carbon nanotubes enhanced cellulose nanocrystals films with tailorable electrical conductivity. Compos Sci Technol 120:1–8. https://doi.org/10.1016/j.compscitech.2015.10.008

Miettinen P, Auvinen S, Kuusipalo J, Haakana S (2015) Validity of traditional barrier-testing methods to predict the achievable benefits of the new generation water based barrier coatings for packaging materials. In: D3 Professional conference proceedings. PTS coating symposium, Munich, Germany, pp 328–342

Moon RJ, Schueneman GT, Simonsen J (2016) Overview of cellulose nanomaterials, their capabilities and applications. JOM 68:2383–2394. https://doi.org/10.1007/s11837-016-2018-7

Nazari B, Kumar V, Bousfield DW, Toivakka M (2016) Rheology of cellulose nanofibers suspensions: boundary driven flow. J Rheol 60:1151–1159. https://doi.org/10.1122/1.4960336

Nelson K, Retsina T, Iakovlev M, van Heiningen A, Deng Y, Shatkin JA, Mulyadi A (2016) American process: production of low cost nanocellulose for renewable, advanced materials applications. In: Madsen LD, Svedberg EB (eds) Materials research for manufacturing. Springer, Berlin, pp 267–302

Osong SH, Norgren S, Engstrand P (2016) Processing of wood-based microfibrillated cellulose and nanofibrillated cellulose, and applications relating to papermaking: a review. Cellulose 23:93–123. https://doi.org/10.1007/s10570-015-0798-5

Pan M, Zhou X, Chen M (2013) Cellulose nanowhiskers isolation and properties from acid hydrolysis combined with high pressure homogenization. BioResources 8:933–943. https://doi.org/10.15376/biores.8.1.933-943

Pereira ALS, do Nascimento DM, Filho Souza, Men de Sá M, Morais JPS, Vasconcelos NF, Feitosa JPA, Brígida AIS, Rosa MDF (2014) Improvement of polyvinyl alcohol properties by adding nanocrystalline cellulose isolated from banana pseudostems. Carbohyd Polym 112:165–172. https://doi.org/10.1016/j.carbpol.2014.05.090

Plackett DV, Letchford K, Jackson JK, Burt HM (2014) A review of nanocellulose as a novel vehicle for drug delivery. Nord Pulp Pap Res J 29:105–118. https://doi.org/10.3183/NPPRJ-2014-29-01-p105-118

Samyn P, Barhoum A, Öhlund T, Dufresne A (2018) Review: nanoparticles and nanostructured materials in papermaking. J Mater Sci 53:146–184. https://doi.org/10.1007/s10853-017-1525-4

Shafiei-Sabet S, Hamad WY, Hatzikiriakos SG (2012) Rheology of nanocrystalline cellulose aqueous suspensions. Langmuir 28:17124–17133. https://doi.org/10.1021/la303380v

Valentini L, Cardinali M, Fortunati E, Torre L, Kenny JM (2013) A novel method to prepare conductive nanocrystalline cellulose/graphene oxide composite films. Mater Lett 105:4–7. https://doi.org/10.1016/j.matlet.2013.04.034